



Microstructure and mechanical properties of mechanically alloyed $\text{Al}_2\text{O}_3/\text{Ti}-\text{Cu}-\text{Ni}-\text{Sn}$ bulk metallic glass composites prepared by vacuum hot-pressing

Hong-Ming Lin^a, Chin-Yi Chen^b, Chien-Yie Tsay^b, Chih-Feng Hsu^c, Pee-Yew Lee^{c,*}

^a Department of Materials Engineering, Tatung University, Taipei, Taiwan

^b Department of Materials Science and Engineering, Feng-Chia University, Taichung, Taiwan

^c Institute of Materials Engineering, National Taiwan Ocean University, 2 Pei-Ning Road, Keelung, Taiwan

ARTICLE INFO

Article history:

Received 2 July 2009

Received in revised form

22 December 2009

Accepted 8 February 2010

Available online 13 February 2010

Keywords:

Mechanical alloying

Bulk metallic glass composite

Supercooled liquid region

Vacuum hot-pressing

Al_2O_3

ABSTRACT

In the present study, $\text{Ti}_{50}\text{Cu}_{28}\text{Ni}_{15}\text{Sn}_7$ metallic glass and its composite powders reinforced with 4–12 vol.% of Al_2O_3 added were successfully prepared by mechanical alloying. In the ball-milled composites, an amorphous matrix with a homogeneous dispersion of Al_2O_3 particles was developed. The metallic glass composite powders were found to exhibit a large supercooled liquid region before crystallization. The presence of Al_2O_3 particles did not change the glass formation ability of the amorphous $\text{Ti}_{50}\text{Cu}_{28}\text{Ni}_{15}\text{Sn}_7$ powders. Consolidation of the as-milled $\text{Ti}_{50}\text{Cu}_{28}\text{Ni}_{15}\text{Sn}_7$ composite powders was performed at a temperature slightly higher than the glass transition temperature under a pressure of ~ 1.2 GPa; using this method, the bulk metallic glass composite discs were prepared successfully. However, partial crystallization of the amorphous matrix during the hot-pressing process was noticed. The fracture strength of consolidated composite compacts was increased with Al_2O_3 additions. The pre-existing particle boundaries may serve as the crack initiation sites which resulted in the brittle failure of the $\text{Ti}_{50}\text{Cu}_{28}\text{Ni}_{15}\text{Sn}_7$ BMG composites.

© 2010 Elsevier B.V. All rights reserved.

1. Introduction

Recently, many techniques have been successfully used to prepare bulk metallic glass (BMG) composites, but most of the research efforts and industrial interests are focused on the different implementations of rapid solidification [1]. However, the preparation of a glassy matrix composite by casting often results in partial crystallization at the interface between the amorphous and ceramic phases. Moreover, the differences in densities or melting points among the raw metallic and particulate materials make it difficult to prepare cast samples.

An alternative method is using a solid-state amorphization process, for instance mechanical alloying (MA), to prepare amorphous powders that are suitable for further compaction and densification. Meanwhile, reinforced particles can be introduced easily into the glassy matrix. As previous investigations have demonstrated, MA has been successfully used to prepare amorphous Cu-based composite powders [2]. However, available literature does not report on the formation of a Ti-based composite powder by the MA process. In the present study, $\text{Ti}_{50}\text{Cu}_{28}\text{Ni}_{15}\text{Sn}_7$ metallic glass powders with

or without Al_2O_3 additions are prepared by MA. These as-milled powders are subsequently consolidated and the mechanical property of these compacts evaluated by Vickers microhardness and compression tests.

2. Experimental procedure

The mixture of the elemental metallic powders nominally composed of $\text{Ti}_{50}\text{Cu}_{28}\text{Ni}_{15}\text{Sn}_7$ (in at.%) was mechanically alloyed with or without the addition of Al_2O_3 powders. The milling was performed in a SPEX 8016 shaker ball mill under an Ar-filled atmosphere. The specific details of the mechanical alloying process are described elsewhere [2]. The as-milled composite powders were consolidated in a vacuum hot-pressing machine to yield bulk samples with a 10-mm diameter and 2-mm thickness. The as-milled powders and hot-pressed BMG composite discs were examined by X-ray diffraction (XRD), differential scanning calorimeter (DSC), scanning electron microscopy (SEM), and transmission electron microscopy (TEM). The Vickers microhardness of the consolidated BMG samples was measured with a Matsuzawa MXT50-UL machine using a static load of 500 g. The compression test was performed by a universal testing machine (Instron 4050) at a strain rate of $1 \times 10^{-4} \text{ s}^{-1}$.

3. Results and discussion

Fig. 1 shows the X-ray diffraction patterns of the $\text{Ti}_{50}\text{Cu}_{28}\text{Ni}_{15}\text{Sn}_7$ sample and of the samples with 4, 8 and 12 vol.% Al_2O_3 additions after 8 h of milling. Only a broad diffraction peak appears around $2\theta = 42^\circ$, indicating that a fully amorphous phase

* Corresponding author.

E-mail address: pylee@mail.ntou.edu.tw (P.-Y. Lee).

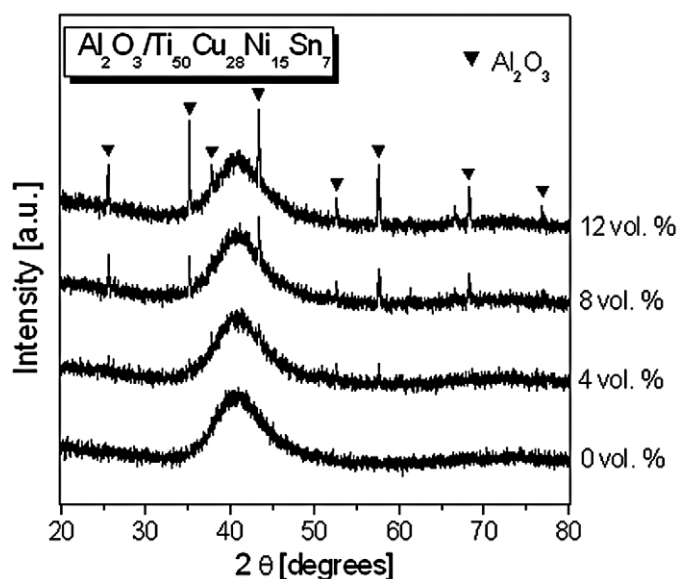


Fig. 1. X-ray diffraction patterns for mechanically alloyed $\text{Ti}_{50}\text{Cu}_{28}\text{Ni}_{15}\text{Sn}_7$ and composite powders after 8 h milling.

has formed for plain $\text{Ti}_{50}\text{Cu}_{28}\text{Ni}_{15}\text{Sn}_7$ alloy powders. In the case of the composite powders, as seen in Fig. 1, the Bragg peaks of the Al_2O_3 are barely detectable in the diffraction patterns for the composite powders of $\text{Ti}_{50}\text{Cu}_{28}\text{Ni}_{15}\text{Sn}_7$ alloy mixed with 4 vol.% Al_2O_3 particles after 8 h of milling. This may be attributed to the low volume fraction of Al_2O_3 particles and their small crystalline size. Hsieh et al. [3] reported that, similarly to what has been observed in this work for the preparation of $\text{Al}_2\text{O}_3/\text{Ni}_{57}\text{Zr}_{20}\text{Ti}_{20}\text{Si}_3$ amorphous-matrix composite, for 10 vol.% Al_2O_3 additions in mechanically alloyed $\text{Ni}_{57}\text{Zr}_{20}\text{Ti}_{20}\text{Si}_3$ amorphous alloys, no Al_2O_3 phase could be detected by XRD after 5 h milling.

A scanning electron microscope was used to examine the cross-sectional view of as-milled composite powders; these SEM images are shown in Fig. 2. As revealed in Fig. 2, for $\text{Ti}_{50}\text{Cu}_{28}\text{Ni}_{15}\text{Sn}_7$ powders with 8 vol.% Al_2O_3 additions, a uniform distribution of fine Al_2O_3 particles within the amorphous matrix was observed at the end of milling. The size distribution ranges from 1 μm to values below 50 nm, which is the resolution limit of the SEM. The composition of the particles was proven to be that of Al_2O_3 by EDX analysis.

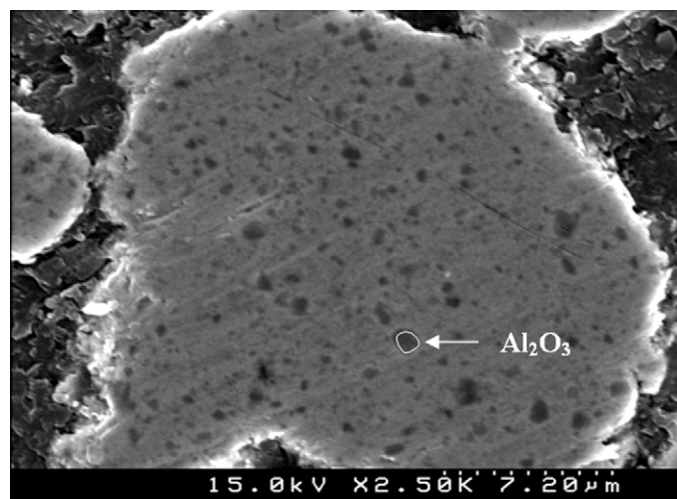


Fig. 2. SEM cross-sectional image of 8 h as-milled $\text{Ti}_{50}\text{Cu}_{28}\text{Ni}_{15}\text{Sn}_7$ composite powders with 8 vol.% Al_2O_3 additions.

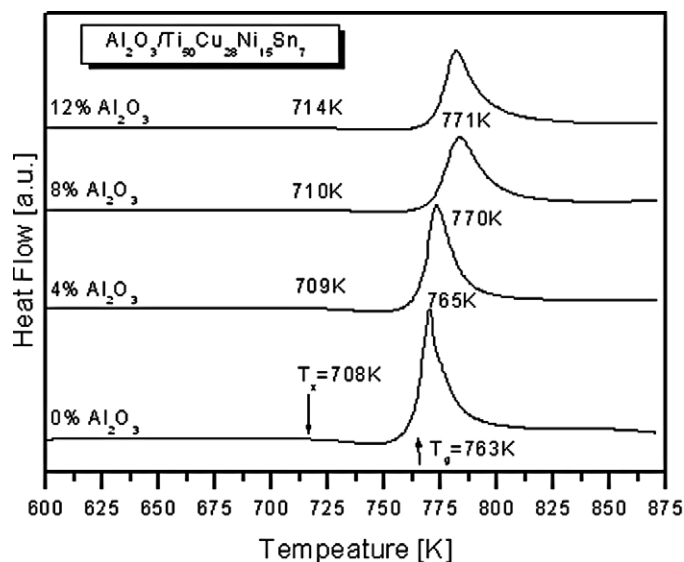


Fig. 3. DSC scans of mechanically alloyed $\text{Ti}_{50}\text{Cu}_{28}\text{Ni}_{15}\text{Sn}_7$ and composite powders after 8 h milling.

Differential scanning calorimetry (DSC) was used to investigate the glass transition and crystallization behaviors of the as-milled powders. The DSC scans of the 8 h as-milled $\text{Ti}_{50}\text{Cu}_{28}\text{Ni}_{15}\text{Sn}_7$ monolithic glass and of the composites with Al_2O_3 particles are shown in Fig. 3. The glass transition (T_g) and crystallization (T_x) temperatures are defined as the onset temperature of the endothermic and exothermic DSC events, respectively. As shown in Fig. 3, the amorphous $\text{Ti}_{50}\text{Cu}_{28}\text{Ni}_{15}\text{Sn}_7$ and $\text{Al}_2\text{O}_3/\text{Ti}_{50}\text{Cu}_{28}\text{Ni}_{15}\text{Sn}_7$ composite powders exhibited similar supercooled liquid regions (ΔT_x , i.e., $T_x - T_g$). Table 1 summarizes the values of T_g , T_x , and ΔT_x for all the samples investigated in the present study. The glass transition temperature and the crystallization temperature of composite powders are slightly higher than those of a single-phase amorphous $\text{Ti}_{50}\text{Cu}_{28}\text{Ni}_{15}\text{Sn}_7$ alloy. These shifts in transition temperatures may be explained by a slight change in the amorphous-matrix composition caused by the dissolution of small amounts of Al and O during mechanical alloying. The activation energy (E_c) for crystallization as determined by the Kissinger Method [4] is also listed in Table 1. No significant difference (<5%) in activation energies was found. Based on the above DSC results, the presence of the Al_2O_3 particles does not dramatically reduce the thermal stability of the $\text{Ti}_{50}\text{Cu}_{28}\text{Ni}_{15}\text{Sn}_7$ amorphous matrix.

Following the DSC results, the 8 h as-milled composite powders were consolidated into a disk by vacuum hot-pressing with a 10-mm diameter and 2-mm thickness. The cross-sectional view of the corresponding disc sample examined by SEM is shown in Fig. 4, illustrating the homogeneous dispersion of the Al_2O_3 particles of submicron size.

In order to observe the microstructure within the bulk metallic glasses, the sample with 8 vol.% Al_2O_3 additions, was examined by transmission electron microscope (TEM). TEM bright field image

Table 1
Thermal stability of amorphous $\text{Ti}_{50}\text{Cu}_{28}\text{Ni}_{15}\text{Sn}_7$ and its composite powders prepared by mechanical alloying.

Composition	Thermal property			
	T_g (K)	T_x (K)	ΔT_x (K)	E_c (kJ/mol)
$\text{Ti}_{50}\text{Cu}_{28}\text{Ni}_{15}\text{Sn}_7$	708	763	55	332
$\text{Ti}_{50}\text{Cu}_{28}\text{Ni}_{15}\text{Sn}_7$ + 4 vol.% Al_2O_3	709	765	56	330
$\text{Ti}_{50}\text{Cu}_{28}\text{Ni}_{15}\text{Sn}_7$ + 8 vol.% Al_2O_3	710	770	60	335
$\text{Ti}_{50}\text{Cu}_{28}\text{Ni}_{15}\text{Sn}_7$ + 12 vol.% Al_2O_3	714	771	57	325

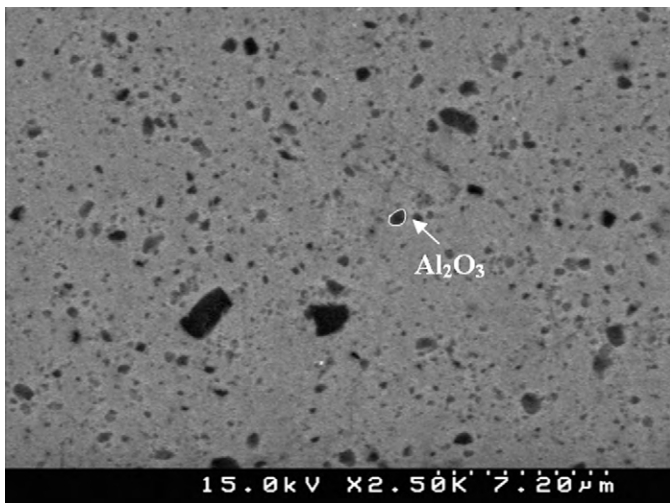


Fig. 4. SEM cross-sectional image of the bulk $\text{Ti}_{50}\text{Cu}_{28}\text{Ni}_{15}\text{Sn}_7$ composite with 8 vol.% Al_2O_3 additions prepared using the 8 h milled composite powder.

is shown in Fig. 5(a), where Al_2O_3 nanoparticles with irregular shapes and sizes ranging from 60 to 400 nm are embedded within the amorphous matrix. The inset shown in Fig. 5(a) presents the selected area diffraction (SAD) pattern taken from the matrix, which shows a typical amorphous pattern characterized by a diffuse halo with limited diffraction spots. In order to examine in more detail the bonding state at the interface between the amorphous and Al_2O_3 phases, high-resolution TEM images were taken at the interface and are shown in Fig. 5(b). The interfacial structure is clearly lacking in pores or voids between the amorphous phase, with its featureless modulated contrast, and the Al_2O_3 phase, with its periodic fringe contrast. This implies that the BMG composite was prepared successfully by hot-pressing the as-milled powders at 723 K under a pressure of 1.2 GPa, with only limited nanocrystallization occurring during consolidation.

Fig. 6 shows compressive stress–strain curves of the composite bulk alloys containing 4, 8, and 12 vol.% Al_2O_3 , together with the data pertaining to the $\text{Ti}_{50}\text{Cu}_{28}\text{Ni}_{15}\text{Sn}_7$ bulk glassy single-phase alloy. As seen in the curves, $\text{Ti}_{50}\text{Cu}_{28}\text{Ni}_{15}\text{Sn}_7$ monolithic glass and the composites with Al_2O_3 particles all deformed elastically and failed without any macroscopic yielding or distinct plasticity. It can be seen that the fracture strength for $\text{Ti}_{50}\text{Cu}_{28}\text{Ni}_{15}\text{Sn}_7$ monolithic glass was 1830 MPa, and increased to 1879, 2112 and 2187 MPa for those with 4, 8, 12 vol.% Al_2O_3 additions, respectively. However, it is also noted the elastic strain of $\text{Ti}_{50}\text{Cu}_{28}\text{Ni}_{15}\text{Sn}_7$ monolithic glass was 2.48% and slightly decreased to 2.08%, 2.01% and 1.86% after adding 4, 8, 12 vol.% Al_2O_3 .

Fig. 7 shows the fracture surfaces of $\text{Ti}_{50}\text{Cu}_{28}\text{Ni}_{15}\text{Sn}_7$ composites containing 8 vol.% Al_2O_3 particles. The fracture surfaces of the composites became very rough, with Al_2O_3 particles distributed uniformly on the surface. A brittle fracture that initiated at the particle boundaries or in the interior of the powder particles was observed in the specimens. It is expected that the existence of Al_2O_3 particles can improve the ductility of the $\text{Ti}_{50}\text{Cu}_{28}\text{Ni}_{15}\text{Sn}_7$ monolithic glass. However, examination of Fig. 7 indicated that the Al_2O_3 particles are detached from the matrix during fracturing of the composite samples. This means the addition of Al_2O_3 has no obvious effect on blocking the propagation of shear band. Choi-Yim et al. [5] have reported that the plasticity of Zr-based bulk metallic glass matrix particulate composites can be improved significantly by using larger reinforcement particles. The mean size of Al_2O_3 particles is about 500 nm, it seen that these nanoscale Al_2O_3 particles cannot restrict shear bands propagation and promote the generation of multiple shear bands. A number of previous studies

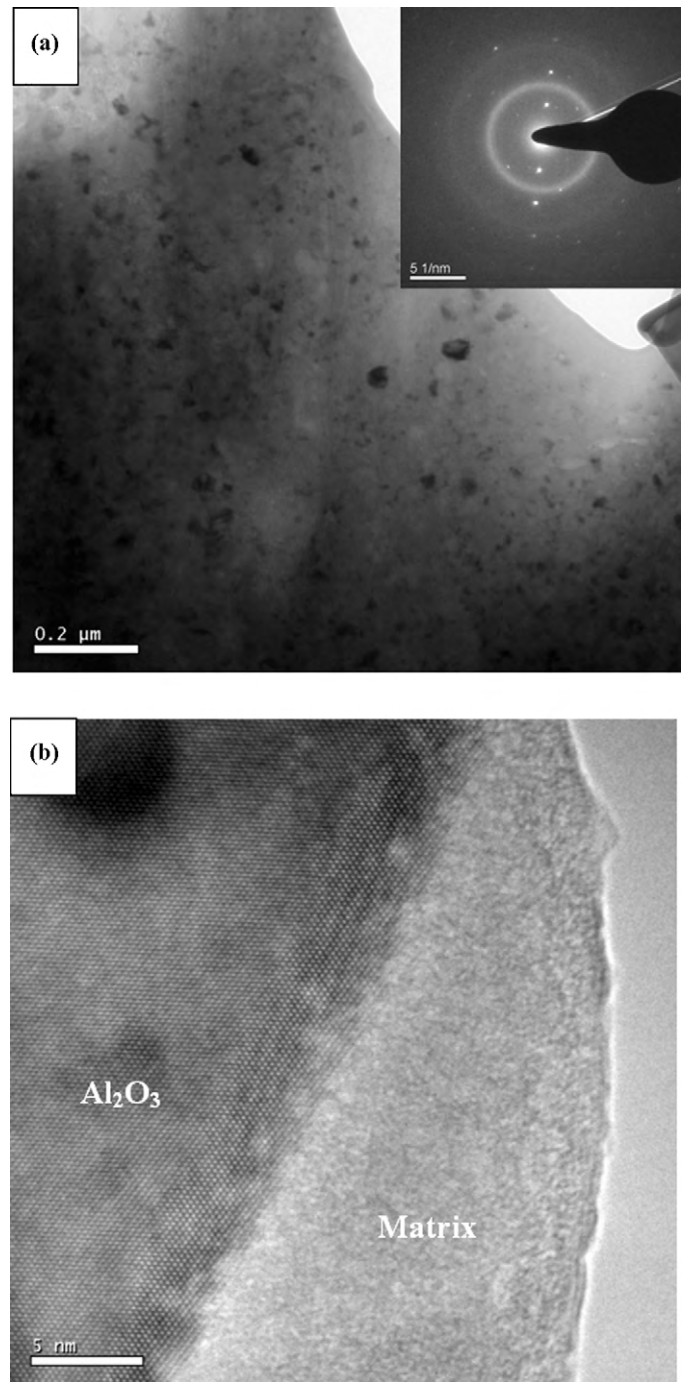


Fig. 5. TEM observation of the consolidated $\text{Ti}_{50}\text{Cu}_{28}\text{Ni}_{15}\text{Sn}_7$ –8 vol.% Al_2O_3 samples. (a) Bright field image and (b) high-resolution micrograph of the interface region.

have prepared bulk metallic glasses by consolidating amorphous alloy powders with different techniques. Under uniaxial compression, the porosity, pre-existing particle boundaries, and interfaces between the nanocrystals and amorphous-matrix mat serve as crack nucleation sites that can propagate and grow rapidly [6–8]. Thus, brittle failure typically occurs before reaching the elastic limit and no plastic deformation is observed. A BMG sample prepared by powder metallurgy suffers from pre-existing crack initiation sites that can propagate and grow rapidly. This failure mechanism differs from the local shear bands of injection-cast BMGs [9]. In the present study, the shapes individual grains, reminiscent of their original powder shapes, can be easily recognized. Since no ductil-

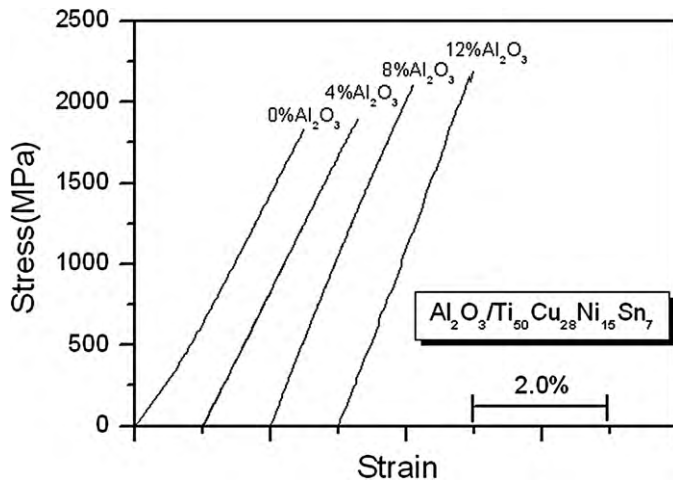


Fig. 6. Compressive stress–strain curves for the consolidated $\text{Ti}_{50}\text{Cu}_{28}\text{Ni}_{15}\text{Sn}_7$ monolithic glass, and the composites with Al_2O_3 particles.

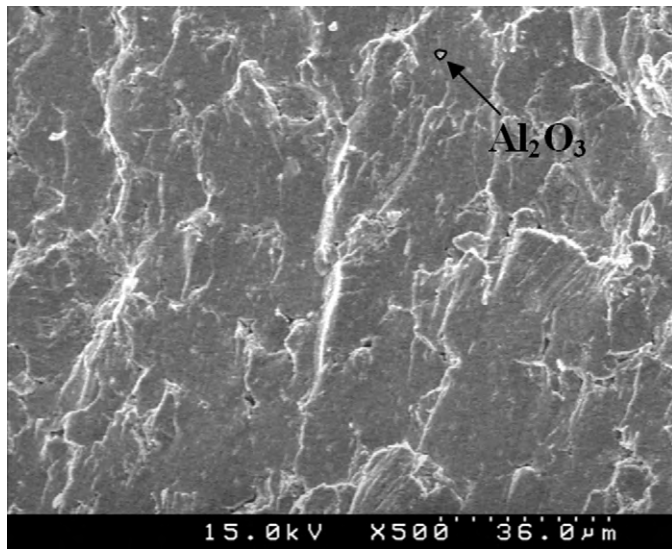


Fig. 7. SEM photographs of fracture surface of containing 8 vol.% Al_2O_3 .

ity was observed in these compacts, it is very likely that complete adhesion between powders had not taken place. Efforts to avoid partial nanocrystallization and to eliminate particle boundaries are underway and will be reported elsewhere.

4. Conclusion

In the present study, $\text{Ti}_{50}\text{Cu}_{28}\text{Ni}_{15}\text{Sn}_7$ metallic glass composite powders were successfully synthesized by the mechanical alloying of powder mixtures of pure Ti, Cu, Ni, Sn and Al_2O_3 after 8 h milling. The metallic glass composite powders were found to exhibit a supercooled liquid region before crystallization. The thermal stability of the amorphous matrix was slightly affected by the addition of the Al_2O_3 particles. BMG composite compact discs were obtained by consolidating the 8 h as-milled composite powders by a vacuum hot-pressing process. The microstructure of $\text{Ti}_{50}\text{Cu}_{28}\text{Ni}_{15}\text{Sn}_7$ BMG with 8 vol.% Al_2O_3 additions exhibited an amorphous matrix embedded with Al_2O_3 nanoparticles ranging from 60 to 400 nm. An increase in fracture strength was achieved for $\text{Ti}_{50}\text{Cu}_{28}\text{Ni}_{15}\text{Sn}_7$ BMG composites with Al_2O_3 additions. The pre-existing particle boundaries may serve as crack initiation sites and be responsible for the appearance of brittle failure in the $\text{Ti}_{50}\text{Cu}_{28}\text{Ni}_{15}\text{Sn}_7$ BMG composites.

References

- [1] A. Inoue, Mater. Sci. Forum 312–314 (1999) 307–314.
- [2] C.K. Lin, Y.L. Lin, J.S. Chen, R.R. Jen, P.Y. Lee, Mater. Sci. Forum 475–479 (2005) 3443–3450.
- [3] J.T. Hsieh, C.K. Lin, J.S. Chen, R.R. Jen, Y.L. Lin, P.Y. Lee, Mater. Sci. Eng. A 375/377 (2004) 820–824.
- [4] H.E. Kissinger, Anal. Chem. 29 (1957) 1702–1706.
- [5] H. Choi-Yim, R.D. Conner, F. Szuets, W.L. Johnson, Acta Mater. 50 (2002) 2737–2745.
- [6] Y. Kawamura, H. Kato, A. Inoue, T. Masumoto, Int. J. Powder Metall. 33 (1997) 50–61.
- [7] M. Takagi, Y. Kawamura, T. Imura, J. Nishigaki, H. Saka, J. Mater. Sci. 27 (1992) 817–824.
- [8] M. Takagi, Y. Kawamura, M. Araki, Y. Kuroyama, T. Imura, Mater. Sci. Eng. 98 (1988) 457–460.
- [9] W.H. Wang, C. Dong, C.H. Shek, Mater. Sci. Eng. R 44 (2004) 45–89.